J Mol Model
DOI 10.1007/s00894-015-2752-8

ORIGINAL PAPER

Calculations of hyperfine coupling constant of copper(II) in aqueous environment. Finite temperature molecular dynamics and relativistic effects

Michal Malček[1] · Lukáš Bučinský[1] · Marián Valko[1] · Stanislav Biskupič[1]

Received: 17 February 2015 / Accepted: 3 July 2015

Abstract The presented paper is focused on the calculation of hyperfine coupling constants (HFCC) of Cu^{2+} ion in water environment. To simulate the conditions of the electron paramagnetic resonance (EPR) experiment in aqueous phase, molecular dynamics using the density functional theory (DFT) was employed. In total three different functionals (BLYP, B3LYP, M06) were employed for studying their suitability in describing coordination of Cu^{2+} by water molecules. The system of our interest was composed of one Cu^{2+} cation surrounded by a selected number (between thirty and fifty) of water molecules. Besides the non-relativistic HFCCs (Fermi contact terms) of Cu^{2+} also the four-component relativistic HFCC calculations are presented. The importance of the proper evaluation of HFCCs, the inclusion of spin-orbit term, for Cu^{2+} containing systems (Neese, J. Chem. Phys. 118, 3939 2003; Almeida et al., Chem. Phys. 332, 176 2007) is confirmed at the relativistic four-component level of theory.

Keywords Copper(II) · Density functional theory · Fermi contact term · Hyperfine coupling constant · Molecular dynamics

Electronic supplementary material The online version of this article (doi:10.1007/s00894-015-2752-8) contains supplementary material, which is available to authorized users.

✉ Michal Malček
michal.malcek@stuba.sk

[1] Institute of Physical Chemistry and Chemical Physics FCFT, Slovak University of Technology, Radlinskeho 9, Bratislava, SK-812 37, Slovakia

Introduction

The coordination geometry and preferred number of coordinating ligands to metal ions in transition metal complexes demonstrate a large degree of variety [1]. A large number of transition metal complexes exhibit a variable number of ligands, most frequently ranging from four to nine. In solution, there exist usually several distinct geometrical arrangements of ligands around a metal ion. These different coordination modes of the complexes are likely to play a critical role in the biological functions of metal-containing enzymes [2]. The release and capture of metal ions at the active metal binding sites of proteins are frequently controlled by a mechanism that is finely tuned by the coordination modes.

Zinc and nickel were studied both experimentally and theoretically in great details [3]. On the other hand, divalent paramagnetic copper ion [herein denoted as copper(II) or Cu^{2+}, for brevity] was theoretically studied less frequently. However, copper is one of the most abundant transition metals in biological systems and coordination compounds containing copper are frequently studied [4–6]. In addition to copper complexes, copper is an integral part of various metalloproteins such as cytochrome c oxidase, tyrosinase and superoxide dismutase.

Since water is the most natural ligand of copper containing binding sites in metalloproteins and generally the most natural environment for solvation of metal cations in biological systems, copper hydration studies are of significant interest for biochemists and biophysicists.

An interesting paper by Stace et al. reported mass spectrometry of the cupric complexes coordinated by water molecules in gas phase [7]. The correlation between the ion intensity and the number of coordinated solvent molecules gives insight into the structures of metal-solvent complexes.

Published online: 18 August 2015

Surprisingly, the maximum intensity was found for copper complexes coordinated by eight molecules of water. Showing that the six-coordination is not the most stable form in the gas phase and/or that the impact of the interaction between molecules in the first and second solvation sphere are of non-negligible importance. However, coordination chemistry of copper in fluid or solid state exhibits the most common coordination number of four, five or six. The crystallographic structure database search [8, 9] containing Cu^{2+} coordinated with four, five and six water molecules has yielded six, six and seventy hits, respectively.

From the experimental point of view, a high angle extended X-ray absorption fine structure (EXAFS) and X-ray absorption near edge structure (XANES) methods have been used very extensively to obtain the first solvation sphere coordination scenario of Cu^{2+} in water and to derive the appropriate Cu-O radial distribution function, respectively. The obtained results range from predicting an equilibrium of a square planar geometry shifted towards a tetragonal pyramid [10], through preferring rather the tetragonal pyramid instead of a symmetric or Jahn-Teller (JT) distorted octahedral symmetry [11] up to the preference of the JT distorted sixfold coordination geometry [12]. Pasquarello et al. [13] have reported an exclusively fivefold coordination geometry, see below. Chaboy et al. [14] have rather proposed that the different results which are obtained by the same techniques, might esteem from a double/multiple channel process. Thus, the measured signal might be a superposition of not only one geometry and needs to account for dynamics of the system. The heat of the X-ray beam might also affect the local equilibrium in the liquid phase, making the determination of the correct coordination number of a real challenge.

The classical picture with the six octahedrally coordinated water molecules to Cu^{2+} (with two bonds elongated due to the Jahn-Teller distortion [15]), which is strongly preferred in the crystal structures, is doubted also by theoretical findings. Pasquarello et al. [13] performed Car-Parrinello (CP) dynamics [16, 17] simulation using non-hybrid DFT of a periodic system consisting of one Cu^{2+} ion and 50 water molecules. Instead of the expected sixfold coordination, the fivefold coordination of Cu^{2+} was obtained. The geometry of the fivefold coordination polyhedron was dynamically changing during the simulation from a square pyramid into a trigonal bipyramid and back, *i.e.* the Berry pseudo-rotation. According to Pasquarello et al. [13], the fivefold coordination was confirmed also by the neutron diffraction methods. Fivefold coordination was also obtained from the (non-hybrid DFT) CP molecular dynamics performed by Amira et al. [18]. On the other hand, Rode and coworkers [19–23] obtained almost exclusively a sixfold coordinated copper(II) with Jahn-Teller distortion of the octahedral ligand field in the presented QM/MM calculations at both Hartree-Fock and B3LYP levels of theory. The only exception found by Rode and coworkers was a resolution of identity BP86 (non-hybrid DFT) calculation [21], which is similar to the BLYP functional calculations employed in the CP simulations [13, 18], and which yielded a fivefold to sixfold coordination ratio of *ca* 60:40 [21]. Concluding that, without the inclusion of exact exchange, the fivefold coordination is becoming more preferred [21]. The molecular dynamics study of Blumberger et al. [24] yielded a coordination number dynamically changing between five and six. For completeness, Almeida et al. [25] have performed a non-hybrid DFT CP dynamics of four-, five- and six-coordinated Cu^{2+} complexes with a subsequent evaluation of the UV-vis-NIR spectra using the obtained CP trajectories showing that the different coordination numbers have a considerable fingerprint impact on the UV and NIR regions of the spectrum, albeit the agreement with experiment in the vis region was unsatisfactory for all considered coordination numbers. Alternatively, Almeida et al. [26] attempted to predict the coordination environment of Cu^{2+} in water upon the calculated and measured [27] electron paramagnetic resonance (EPR) parameters. It was concluded [26] that the more favored coordination number in the first solvation sphere of Cu^{2+} was five with square-pyramidal geometry. This was based on the comparison of the theoretical and experimental g-tensor values and hyperfine coupling constants (HFCC). The hyperfine coupling constant (A_{iso}) calculations of Almeida et al. accounted for the non-relativistic Fermi contact term (A_{FC}), the spin-dipolar contributions (A_{SD}) [26, 28] as well as for the spin-orbit contributions (A_{SO}) [29]. It has been shown [26, 29] that the spin-orbit contributions are crucial for the hyperfine coupling constant of transition metal complexes and they damp the non-relativistic Fermi contact term. The spin-dipolar contributions are actually traceless so these have no real impact on A_{iso} HFCC.

The aim of presented work is the calculation of Fermi contact terms (A_{FC}) and/or hyperfine coupling constants (A_{iso}) of copper(II) in water, approaching the conditions of the liquid phase EPR experiment. First of all, the method of molecular dynamics (MD) [30] is utilized, offering a unique approach to study the time dependent behavior of molecular systems and to involve explicitly the presence of solvent molecules. Previous molecular dynamics simulations (MDS) have been based on either non-hybrid or hybrid functionals leading to either sixfold or fivefold coordination of copper, respectively. Herein, we are accounting besides the mentioned functional types also for a meta-hybrid functional to study the correlation between the choice of a functional and the coordination of Cu^{2+} in water environment. Secondly, to assess the experimental HFCCs of copper(II) in a rigor way, the inclusion of a relativistic Hamiltonian so

the proper treatment of the hyperfine coupling operator is required [28, 29, 31–35]. Herein, the four-component relativistic (REL) evaluation of the HFCC has been utilized [33–35] as implemented in the ReSpect code [36]. At this place, it is also worth to note that the hyperfine coupling in the experimental EPR data of Cu^{2+} in water is not resolved at all at the room temperature and that the samples have to be frozen to obtain the hyperfine structure in the measured EPR signal [27]. Thus, it might be interesting to see whether the MD study and/or relativistic effects are capable of mimicking the smearing of the hyperfine interaction of copper(II) (Cu^{2+}) in water at room temperature.

The paper is subdivided as follows: "Computational details" of the calculations are presented at first. The following "Results & discussions" section is split into two parts. The first subsection is focused on the MDS of Cu^{2+} explicitly solvated by water molecules. The impact of the choice of the DFT functional and/or basis set quality on the first solvation sphere geometry and coordination number are studied. The NR Fermi contact terms (A_{FC}) as well as the REL HFCCs (A_{iso}) of copper(II), based on the geometries obtained from the MDS, are considered subsequently.

Computational details

Starting first hydration sphere geometries of Cu^{2+} were chosen according to the work of Almeida et al. [26], a five-coordinated square pyramidal complex and a six-coordinated octahedral complex with Jahn-Teller distortion. The chosen geometries of the $[Cu(H_2O)_5]^{2+}$ and $[Cu(H_2O)_6]^{2+}$ complexes were reoptimized at the BLYP [37, 38], B3LYP [37, 39–41] and M06 [42] levels of theory, employing standard basis sets 6-31G, 6-31G* [43, 44], 6-311G** [45, 46] and the uncontracted cc-pVDZ basis set [47, 48] (denoted as UDZ). All geometry optimizations accounted for the Polarizable Continuum solvent Model (PCM) [49, 50] of water and were performed in Gaussian 09 package [51].

The initially sixfold coordinated system for the MDS is based on the B3LYP/6-311G** geometry of the $[Cu(H_2O)_6]^{2+}$ octahedral complex (with Jahn-Teller distortion) which was subsequently solvated with 24 molecules of water (denoted as I6 for "initially six-coordinated"). The initially fivefold coordinated system for the MDS is based on the B3LYP/6-311G** optimized $[Cu(H_2O)_5]^{2+}$ square pyramidal complex and was solvated with 25 molecules of water (denoted as I5 for "initially five-coordinated"). The solvation was performed in Gromacs package [52]. The number of solvent molecules in the box ($10 \times 10 \times 10$ Å^3) was adjusted to obtain approximately the density of water at room temperature. The coordinates of the solvated system were used as the input for the DFT MD calculations.

The MDSs were performed at the BLYP [37, 38], B3LYP [37, 39], and M06 [42] levels of theory, employing 6-31G and 6-31G* basis sets. All these MDSs were carried out in NWChem package [53]. Berendsen thermostat [54] was employed and the temperature was set to 100 K to heat, relax and temper the system using the time steps of 0.0001, 0.0005 or 0.001 ps at the M06/6-31G level of theory (the time step has been varied to test the stability of the thermostat as a compromise between accuracy and the length of the time step). The subsequent M06/6-31G MDS step was performed without temperature relaxation at 200 K with a time step of 0.001 ps. Finally, the 300 K MDSs of preheated I5 and I6 systems for a chosen functional (M06, BLYP, B3LYP) and basis set (6-31G or 6-31G*) were performed with the time step 0.001 ps. The full time durations of the MDSs were from the interval 10 - 13.5 ps for the I5 and I6 systems. Additional M06/6-31G MDSs of I5 and I6 systems were performed at the temperature of 350 K, to compare the motion of molecules and the dynamic changes of the coordination number in the first solvation sphere at two different temperatures. The time duration of these additional MDSs was 4 ps.

Furthermore, a larger system containing sixfold octahedral complex $[Cu(H_2O)_6]^{2+}$ solvated with additional 43 molecules of water has been prepared in Gromacs package (denoted as I6L). Short MDSs (2-4 ps) employing M06/6-31G* and B3LYP/6-31G* levels of theory at 300 K have been performed for the I6L system. Each of the I6L MDSs was preheated independently (0.25 ps at 100 K, 0.25 ps at 200 K and 0.5 ps at 100 K and 0.5 ps at 200 K for M06/6-31G* and B3LYP/6-31G* setups, respectively). The aim of these additional calculations was to critically inspect results (coordination number of the first solvation sphere) obtained from the MDSs of the I5 and I6 $[Cu(H_2O)_{30}]^{2+}$ systems.

The complete set of geometries from all 300 K MDSs are provided in the "Supplementary material" in the form of xyz files and denoted as: System_DFT-functional_Basis-set.xyz (*e.g.* I6_B3LYP_6-31G.xyz).

Distribution functions of Cu-O distances from the MDSs of the solvation bulk were calculated according to the following formula:

$$g_{Cu-O} = \frac{P}{\rho 4\pi r^2 dr} \quad (1)$$

where P is the probability of finding an oxygen atom in the element dr at the distance r from copper atom (number of oxygen atoms divided by the number of frames), ρ is the number density (particularly 0.0334 Å^{-3}, which corresponds exactly to 1000 kg.m^{-3}) and the element dr was set to 0.1 Å.

Non-relativistic B3LYP/6-311G** calculations of the Fermi contact terms (A_{FC}) for copper(II) from the MD trajectories were performed using the NWChem package. The

MD geometries of every twentieth step were used, from the last 8 ps of the I5 and I6 B3LYP/6-31G and M06/6-31G MDSs at 300 K ($[Cu(H_2O)_{30}]^{2+}$ systems). In the case of B3LYP/6-31G simulations, only the geometry of the first solvation sphere were taken into account in the A_{FC} calculations. On the other hand, in the case of the M06/6-31G trajectories three types of A_{FC} calculations were performed: the first one considered exclusively the first solvation sphere of coordination polyhedron; the second one considered the full MD geometries; and the last one considered again the first solvation sphere of coordination polyhedron but with the inclusion of COSMO (COnductor-like Screening MOdel) [55] solvent model of water.

Relativistic four-component (REL) calculations of HFCCs of copper(II) have been performed using the ReSpect code [36]. Theoretical background on the REL calculations employed within this work can be found in the works of Malkin and coworkers [33–35]. Importantly, Dirac-Kohn-Sham formalism has been employed [34], hand in hand with the finite size nucleus effects (Gaussian nucleus model) [35, 56]. The B3LYP functional [37, 39–41] and uncontracted cc-pVDZ basis set [47, 48] have been employed. Because of the larger demands of the REL calculations, only every 200^{th} first solvation sphere geometry was employed for the same time interval of the last 8 ps of the 300 K MDSs of I5 and I6 systems (involving M06/6-31G and B3LYP/6-31G trajectories).

Results & discussions

Molecular dynamics simulations

This subsection is devoted to the results and data analysis from molecular dynamics simulations (MDS). The temperature and energy profiles from the M06/6-31G MDS of I5 and I6 systems are shown in Fig. 1. One can see from Fig. 1, that both the temperature and energy profiles of the systems are without any excessive oscillations, meaning that the relaxation times and equilibration periods for the 100 K stepwise temperature raise as well as thermostatization are appropriate for the system under study. Furthermore, the shorter simulation times (which did not exceed 15 ps for I5 and I6 systems) are a compromise to achieve reliable results for the second solvation sphere effects accounted for in the MDSs of the I5 and I6 bulks. Long simulation times may lead to deformations of the bulk and an inappropriate description of second solvation sphere interaction with molecules in the first solvation sphere. It is obvious from Fig. 1a and b, that with the higher temperature and larger length of the time step the temperature oscillations are becoming larger. This effect is well documented in the literature [57]. The total energy has relaxed into a *dynamic equilibrium* after *ca* 0.5 ps of the initial 100 K MDS for both I5 and I6 systems, see Fig. 1c and d, respectively. This energy stabilization can be assigned to: geometry relaxation due to inter- / intra-molecular forces and the cavitation of the system closely related to minimization of the outer surface of the bulk. (The solvation box from Gromacs package [52] changes into a spherically shaped cavity.) After 1 ps of M06/6-31G MDS the DFT energies of both I5 and I6 systems oscillate around -3931.2 a.u., see Fig. 1c and d. Although, the absolute value of energy depends on the choice of functional and basis set, the temperature and energy profiles of the remaining 300 K MDSs are showing exactly the same behavior as found for the M06/6-31G MDSs.

Time evolution of Cu-O bond distances for the $[Cu(H_2O)_{30}]^{2+}$ I5 and I6 MDS at different levels of theory are compiled in Fig. 2. The coordination in the first solvation sphere (for both I5 and I6 systems) does not change during the first 3 ps of M06/6-31G MDS at 100 and 200 K, see Figs. 2a and b. After heating the system to 300 K, the I5 system is changing its coordination number from five to six at *ca* 3.2 - 3.5 ps of the M06/6-31G MDS, see Fig. 2a. On the other hand, the I6 M06/6-31G trajectory (see Fig. 2b) keeps the six-coordinated first solvation sphere coordination, although the Cu-O bond distances (water molecules) are oscillating between the first and second solvation sphere. One water molecule (represented by the dashed line) of the I6 system is leaving the first solvation sphere at the time *ca* 9.5 - 10 ps during M06/6-31G MDS, but is almost immediately replaced by another water molecule (represented by the dotted line), see Fig. 2b. Hence it can be concluded, that the M06/6-31G MD bulk simulation of the I5 and I6 clusters at 300 K prefers the sixfold coordination polyhedron rather than the fivefold one. This is in agreement with the works of Rode and coworkers [19–23] who report a sixfold coordination of the first solvation sphere of Cu^{2+} in aqueous environment. Furthermore, the I5 M06/6-31G trajectory supports also the Jahn-Teller distortion in the octahedrally coordinated first solvation sphere. On the other hand, I6 M06/6-31G trajectory recovers partially the features of a dynamic equilibrium between a fivefold and a sixfold coordination in the first solvation polyhedron which is shifted towards the sixfold coordination and was reported also in the MD study of Blumberger et al. [24]. The number of water molecules in the first solvation sphere of Cu^{2+} (see in Table 1) reflects closely the behavior of Cu-O bond lengths compiled in Fig. 2.

The Cu-O evolution of bond distances from B3LYP MDS of I5 and I6 are quite similar for both basis sets used (6-31G and 6-31G*), see Fig. 2e, f, g and h. All these four MDS trajectories prefer the fivefold coordination polyhedron, what is an opposite result to the M06/6-31G MDSs as well as to the works of Rode and coworkers [21–23].

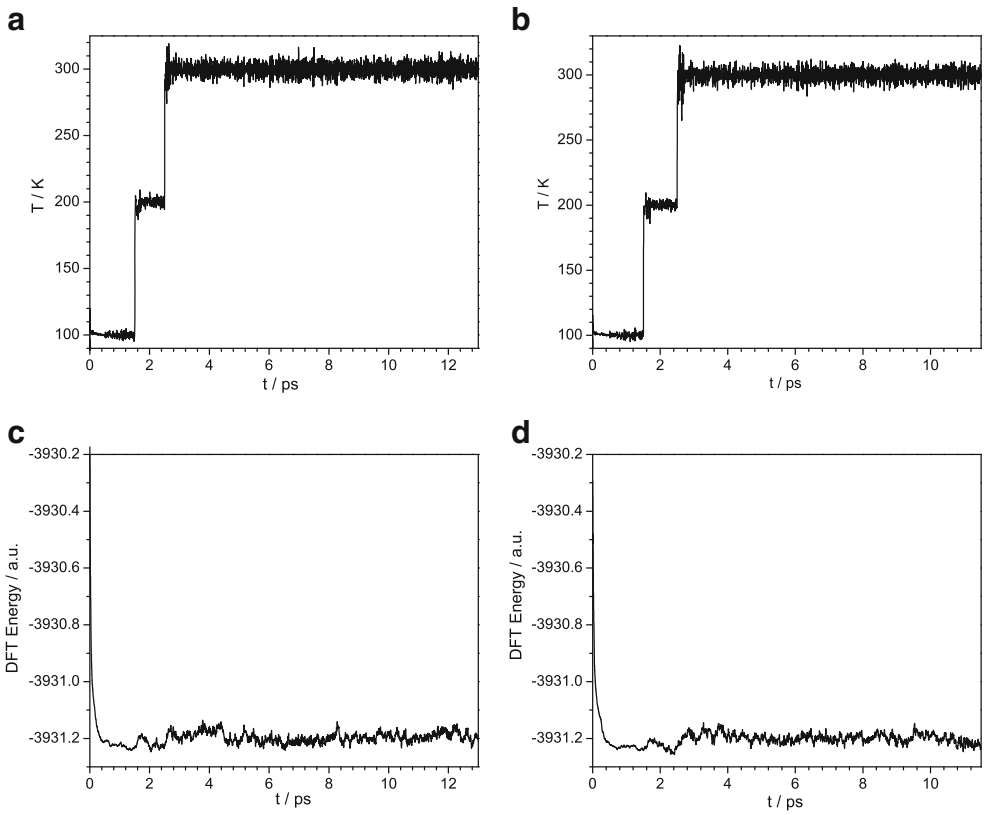

Fig. 1 Temperature (*up*) and energy (*down*) profiles of the M06 MD simulations of systems I5 (*left*) and I6 (*right*)

Thus, the choice (quality) of basis set is a further important factor, which has to be taken into consideration (Rode et al. [21–23] have used the B3LYP functional, but a larger double-ζ basis set). On the other hand, this result is in agreement with the CP MD studies of Pasquarello [13] and Amira [18]. While the I5 system is keeping its five coordination during the whole B3LYP/6-31G and B3LYP/6-31G* MDSs (see Fig. 2e and g), one water molecule in I6 system (the dashed line) is leaving the first solvation sphere at the beginning of B3LYP/6-31G and B3LYP/6-31G* MDSs (see Fig. 2f and h) and the I6 system is becoming fivefold coordinated. Nevertheless, one can see a short presence of the sixfold coordination of Cu^{2+} in the I6 B3LYP/6-31G* MDS trajectory at the time of *ca* 8, 9 and 10.5 ps, see Fig. 2h. BLYP/6-31G MDSs, of both I5 and I6 systems, prefer the fivefold coordination as well, see Fig. 2c and d. In the first half of BLYP MDS trajectory of I6, there is one water molecule (the dashed line) migrating between the first and second solvation sphere, but in the second half of this MDS the system is stable and five coordinated (see Fig. 2d). Interestingly, the fivefold coordination of I5 system during the BLYP MDS is perturbed at the time *ca* 7.5 - 11 ps. In this time period, there are only four molecules of water in the first solvation sphere, see Fig. 2c. This perturbation can be caused by the missing Hartree-Fock exchange part in the BLYP functional (*i.e.* non-hybrid DFT functional).

To allow for a further consistency check of the results, the M06 and B3LYP MDSs have been performed for the I6L system, using the 6-31G* basis set and the simulation bulk contained 49 water molecules in total (initial cluster was a sphere with a radius of 6.75 Å and density of liquid water). It is confirmed that the sixfold and/or fivefold coordination of Cu^{2+} by water molecules is still preferred in the M06/6-31G* and/or B3LYP/6-31G* MDSs of I6L cluster, respectively (see Fig. 3). Another consistency check has been made by the comparison of Cu-O bond distances obtained for BLYP, B3LYP and M06 optimized geometries and using different basis sets (6-31G, 6-31G*, 6-311G** and UDZ), see Table 1. Although one can see quantitative differences in the bond lengths, no qualitative changes can be found. It can be merely concluded that the fivefold geometries are more sensitive to the choice of the functional and/or basis set (see for instance the 6-311G** results). Nevertheless, for the MDSs no qualitative change of the results are observed due to the size of the system and/or presence of polarization functions in the basis set. In addition, the average bond lengths for the BLYP and B3LYP MDS trajectories agree more with the appropriate fivefold coordinated optimal geometries (I5), while for M06 trajectories the average is closer to sixfold coordinated one (I6).

Radial distribution functions $g_{Cu-O}(r)$ (see Eq. 1) of M06/6-31G and B3LYP/6-31G MDSs for both I5 and I6

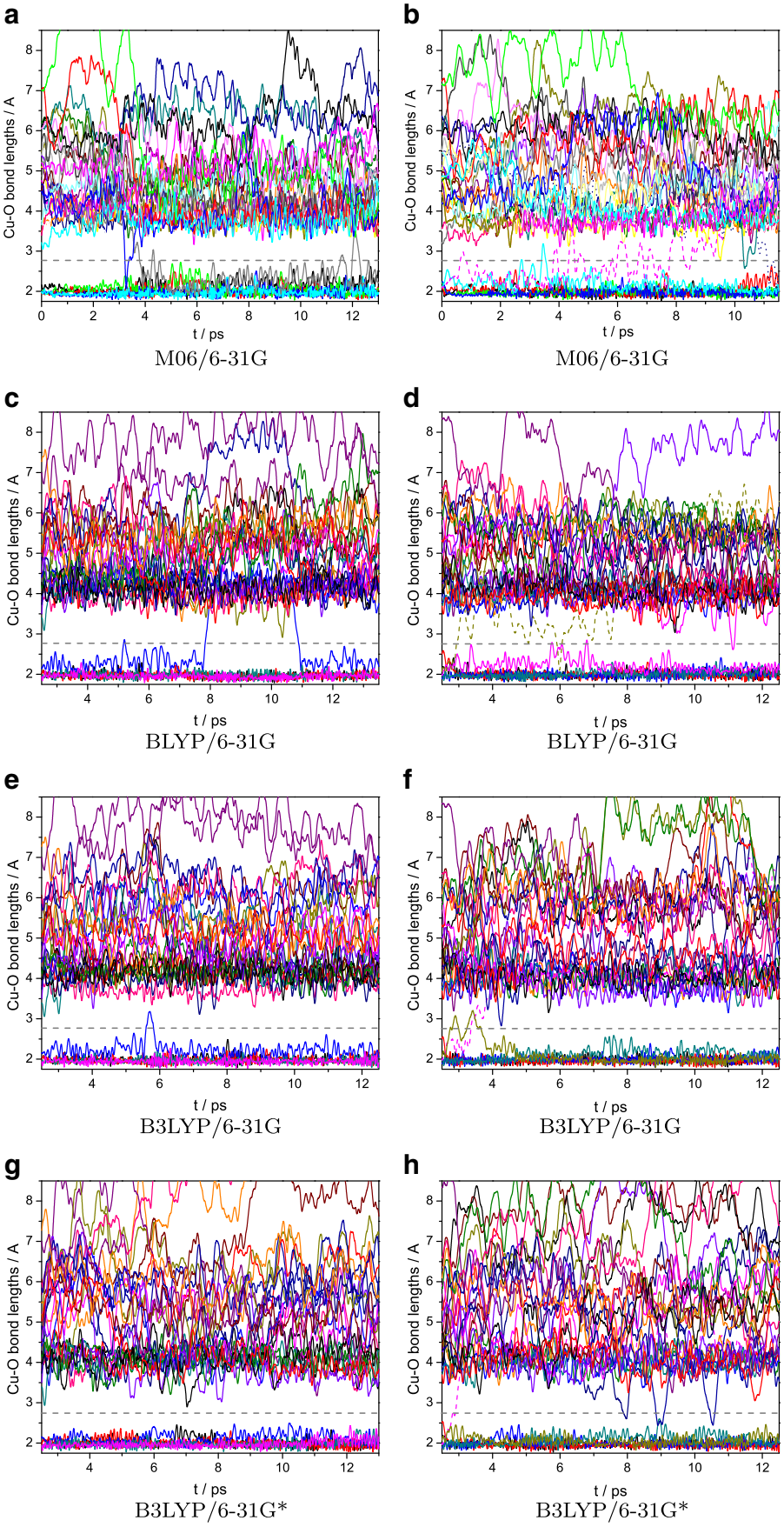

Fig. 2 Time evolutions of Cu-O bond distances of the MD simulations at 300 K of systems I5 (*left column*) and I6 (*right column*) for particular DFT functional and basis set. The dark gray straight dashed line at distance 2.75 Å represents a formal border between the first and second solvation sphere of Cu^{2+}

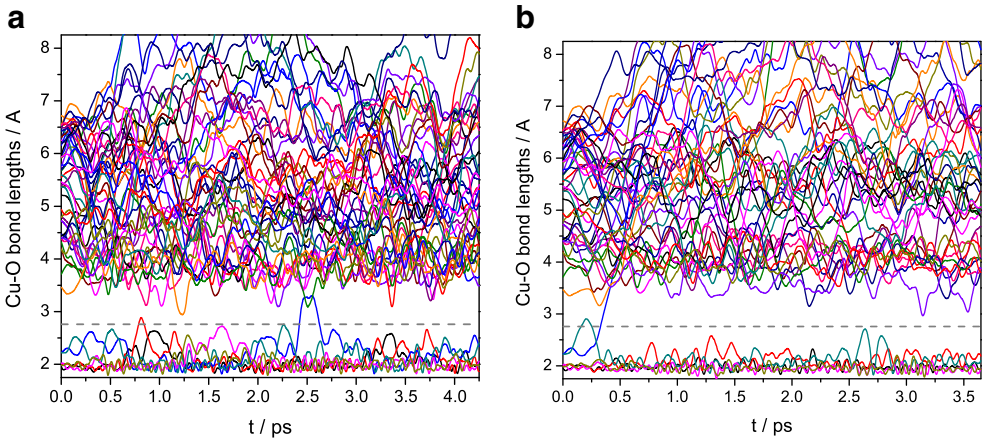

Fig. 3 Time evolutions of Cu-O bond distances of I6L system for M06/6-31G* (*left*) and B3LYP/6-31G* (*right*) MD simulations at 300 K. The dark gray straight dashed line at distance 2.75 Å represents a formal border between the first and second solvation sphere of Cu^{2+}

Table 1 Table of Cu-O bond lengths of optimized complexes, average Cu-O bond lengths and average coordination numbers obtained from MDSs of I5 and I6 at 300 K for different basis sets and DFT functionals

DFT functional:	BLYP	B3LYP	M06	BLYP	B3LYP	M06
System under study:	$[Cu(H_2O)_5]^{2+}$			$[Cu(H_2O)_6]^{2+}$		
Optimized bond lengths						
6-31G	2.114	2.064	2.074	2.253	2.241	2.232
	1.998	2.000	1.978	1.988	2.006	1.985
	1.960	1.946	1.939	1.986	2.006	1.979
6-31G*	2.105	2.109	2.049	2.257	2.224	2.226
	2.040	2.005	2.033	1.975	1.976	1.991
	1.969	1.953	1.942	1.975	1.975	1.986
6-311G**	2.232	2.109	2.184	2.261	2.224	2.222
	1.988	2.003	1.963	1.992	1.974	1.991
	1.987	1.950	1.944	1.991	1.973	1.978
UDZ	2.225	2.168	2.167	2.261	2.257	2.250
	2.048	1.998	1.988	1.992	1.999	2.018
	2.024	1.993	1.968	1.991	1.999	1.996
System under study:	I5			I6		
Average bond lengths						
6-31G	2.02±0.15	2.02±0.15	2.11±0.26	2.05±0.14	2.05±0.16	2.13±0.28
6-31G*		2.02±0.11			2.02±0.11	
Average coordination number[a]						
6-31G	4.681	4.968	5.749	5.009	4.998	5.372
6-31G*		5.000			5.053	
Average coordination number[b]						
6-31G	4.717	4.977	5.849	5.055	5.021	5.498
6-31G*		5.000			5.111	

All bond lengths are in Ångströms

[a]Cu-O radius 2.60 Ångströms

[b]Cu-O radius 2.75 Ångströms

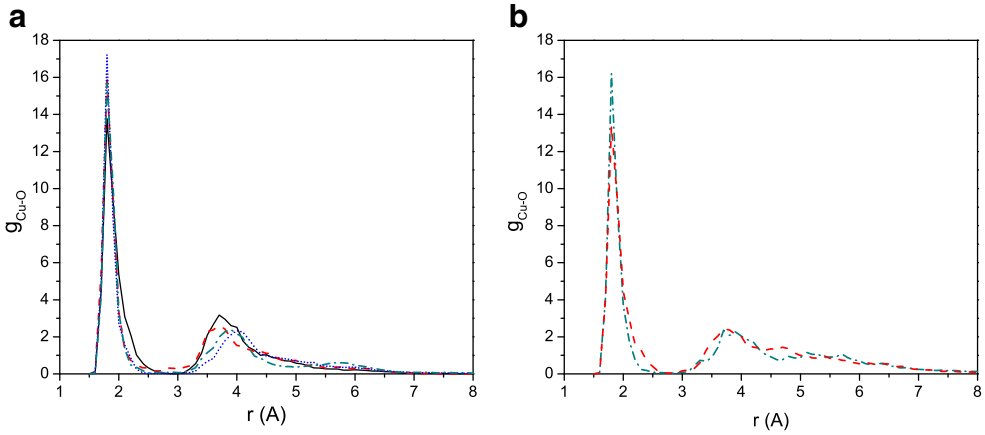

Fig. 4 MDS distribution functions (at 300 K) based on Eq. 1. The left picture **a** is related to the original I5 and I6 systems, particularly: *solid line* is representing the I5 M06/6-31G system, the *dashed line* the I6 M06/6-31G system, *dotted line* the I5 B3LYP/6-31G system and *dash-dot line* the I6 B3LYP/6-31G system. The right picture **b** is related to the I6L cluster, where *dashed line* is representing the M06/6-31G* MDS and *dash-dot line* the B3LYP/6-31G* MDS

systems are shown in Fig. 4a (including I6L M06/6-31G* and I6L B3LYP/6-31G* results in Fig. 4b). In the case of the I5 and I6 systems is the position of the distribution function very similar for either M06 six coordinated or B3LYP five coordinated trajectories. The only difference is in the height of the I5 M06 trajectory which is lower comparing to the remaining three trajectories, and this first solvation sphere peak has a wider tail, both due to JT distortion (2.0 - 2.5 Å). Motion of one water molecule between the first and second solvation sphere of I6 M06 MDS trajectory (see Fig. 2) contributes to the non-zero value of $g_{Cu-O}(r)$ in the range *ca* 2.5 - 3.0 Å. In the case of $g_{Cu-O}(r)$ for the I6L systems, one can also identify a wider tail and a lower first solvation maximum of the I6L M06/6-31G* six coordinated trajectory due to JT distortion, see Fig. 4b. The five coordinated I6L B3LYP/6-31G* trajectory has a similar shape in the first solvation bond region with the particular B3LYP/6-31G trajectories of the I5 and I6 systems. The shape of $g_{Cu-O}(r)$ in the second solvation sphere has a proper behavior for the I6L systems in comparison to the default I5 and I6 MDSs. The larger system naturally accounts for a more complete description of the second solvation sphere.

In the case of I5 and I6 systems heated to 350 K, the situation in the M06/6-31G MDSs of the first solvation sphere is different comparing to the particular 300 K MDSs. The evolution of M06/6-31G Cu-O bond distances at 350 K is shown in the Fig. 5. Especially the I6 system is dynamically changing the number of solvent molecules in the first solvation sphere between five and six, see Fig. 5b. Particularly, one molecule of water (represented by the dashed line) is migrating between the first and second solvation sphere during the 4 ps of the 350 K MDS. In the case

Table 2 Table of A_{FC} values of optimized complexes, average values of NR A_{FC} and REL A_{iso} (including also their standard deviations) using the geometries from MD simulations of I5 and I6 systems

System under study	I5	I6
A_{FC} for optimized (B3LYP/6-311G**) complexes / *Gauss*	−99.727	−88.100
A_{FC} for optimized (B3LYP/UDZ) complexes / *Gauss*	−98.749	−87.600
Average A_{FC} (NR-B3LYP/6-311G**) / *Gauss*		
$[Cu(H_2O)_6]^{2+}$[a]	−83.6±10.6	−88.2±8.9
$[Cu(H_2O)_6]^{2+}$ + COSMO[a]	−83.7±11.0	−87.9±9.6
$[Cu(H_2O)_{30}]^{2+}$[a]	−83.0±13.5	−87.6±11.8
$[Cu(H_2O)_5]^{2+}$[b]	−88.2±9.2	−86.7±9.1
Average A_{iso} (REL-B3LYP/UDZ) / *Gauss*		
$[Cu(H_2O)_6]^{2+}$[a]	−12.7±13.0	−21.5±11.8
$[Cu(H_2O)_5]^{2+}$[b]	−15.6±12.9	−15.3±13.6

All values are related to Cu^{2+} and are given in Gauss

[a]obtained from M06/6-31G MDS

[b]obtained from B3LYP/6-31G MDS

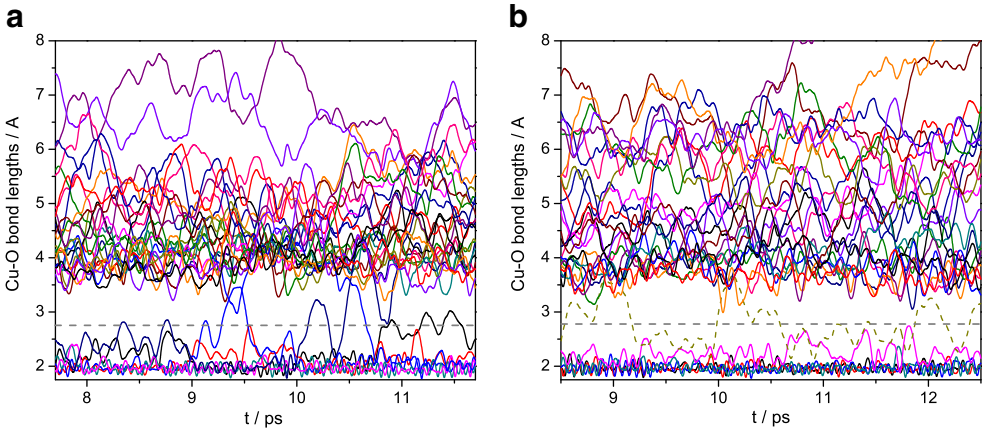

Fig. 5 Time evolutions of Cu-O bond distances of M06/6-31G MD simulations of systems I5 (*left*) and I6 (*right*) at 350 K. The *dark gray straight dashed line* at distance 2.75 Å represents a formal border between the first and second solvation sphere of Cu^{2+}

of I5 system, such motion is not observed in the beginning of the simulation (see Fig. 5a), but from time of 9 ps there is also a noticeable exchange of solvent molecules between the first and second solvation sphere. Based on the above, we may conclude that the preferred coordination number is dynamically changing between a six and five at the higher temperature. Furthermore, we have shown that the sixfold vs. fivefold coordination dynamics is found strongly temperature dependent.

Fermi contact terms and relativistic hyperfine coupling constants

Before considering the Fermi contact terms (A_{FC}) obtained from MDS geometries, A_{FC} values for the B3LYP/6-311G** and B3LYP/UDZ optimized structures of $[Cu(H_2O)_5]^{2+}$ and $[Cu(H_2O)_6]^{2+}$ complexes are worth to be mentioned briefly, see in Table 2. The obtained A_{FC} values are very similar to each other for both used basis sets (the differences are smaller than 1 % for each complex, see Table 2). The calculated B3LYP/6-311G** values of A_{FC} are −99.7 Gauss for $[Cu(H_2O)_5]^{2+}$ and −88.1 Gauss for $[Cu(H_2O)_6]^{2+}$. Fermi contact terms calculated by Almeida et al. [26] at the B3LYP level of theory are −109.9 and −106.5 Gauss in the case of $[Cu(H_2O)_5]^{2+}$ (denoted as "I" in the original paper [26]) and $[Cu(H_2O)_6]^{2+}$ (denoted as "C_i" in the original paper [26]), respectively. These values are larger comparing to our calculated B3LYP/6-311G** values of A_{FC}. These differences can be merely assigned to the different basis sets (including extra tight s-type functions) used for the A_{FC} calculations in Almeida et al. [26]. The optimized Cu-O bond lengths reported in Almeida agree well with the structures obtained in this work. For instance, in the case of the $[Cu(H_2O)_6]^{2+}$ complex are the obtained B3LYP/UDZ Cu-O bond lengths the same as in Almeida et al. [26], i.e. 2.00 Å / 2.26 Å for equatorial/axial directions, respectively.

The time evolutions of the NR A_{FC} values of Cu^{2+} based on the I5 and I6 MDS geometries are presented for both studied systems in Fig. 6. A_{FC} values of five coordinated Cu^{2+} (Fig. 6a and b) were obtained from B3LYP/6-31G MDS and A_{FC} values of six coordinated one (Fig. 6c – f) were obtained from M06/6-31G MDSs of I5 and I6 systems. In the case of the six coordinated Cu^{2+}, the solid line and the dashed line are corresponding to each other quite well (representing the first solvation sphere complex only and the full system, respectively). The larger differences between the two A_{FC} dependencies are found only in the regions of some of the local minima/maxima of the A_{FC} time evolution, see Fig. 6c – f. The "COSMO" A_{FC} values (represented by the blue dots) are either laying on the solid line or can be found between the solid and dashed lines in the regions with larger deviation between A_{FC} of the first solvation sphere and the full system, respectively. Thus, COSMO model is able to simulate the solvation effects of the second solvation sphere quite well. The final NR average values of Fermi contact terms for the obtained MD trajectories are presented in the Table 2. Considering Table 2 one can see that the second solvation sphere has only small contribution (less than 1 %) to the average value of Fermi contact term. According to these results, one can consider A_{FC} calculations of such large clusters as ineffective, when taking into account the significantly higher computational demands. In addition, the negligible impact of the second solvation sphere molecules on the A_{FC} values shows that small deviations in the composition of the entire MD ensemble during the simulation will not lead to dramatic errors in the averages of the hyperfine coupling constants. This is in agreement with experiment. Due to the limited delocalization of metal spin densities over the set of directly coordinated ligands, it is rational to assume that the second solvation sphere will have a negligible impact on A_{FC}. All of the average NR A_{FC} values for the I5 and I6 systems (regardless of coordination number) are within the interval of their standard deviations. The differences

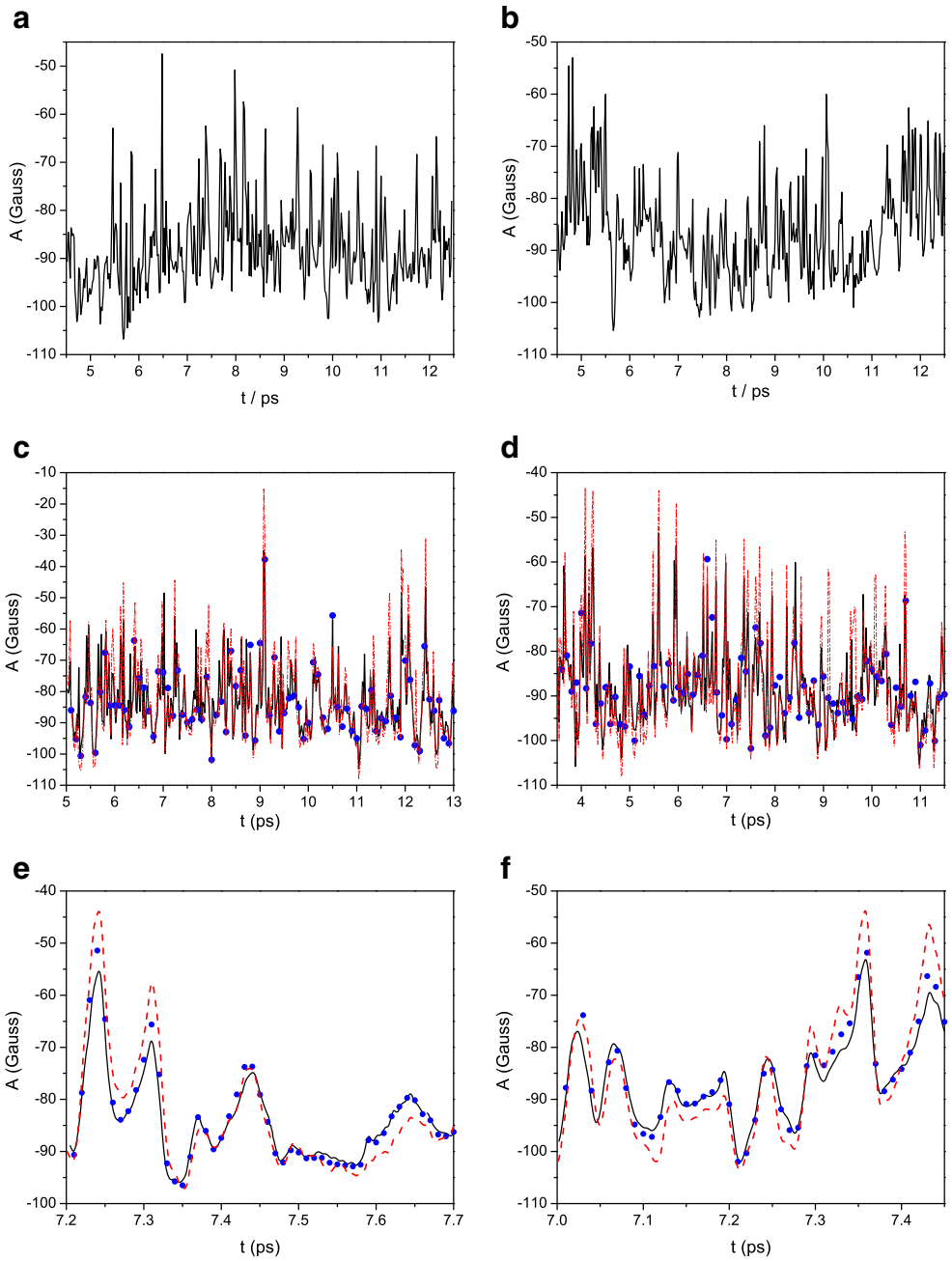

Fig. 6 Time evolutions of NR B3LYP/6-311G** Fermi contact terms (A_{FC}) of copper(II) of systems I5 (*left*) and I6 (*right*). Two upper time dependencies (**a**, **b**) are related to the five coordinated copper(II) from B3LYP/6-31G MDS, two middle ones (**c**, **d**) are related to six coordinated copper(II) from M06/6-31G MDS and the last line (**e**, **f**) offers a closer look on the M06/6-31G MDS based results. In here, the *solid line* is representing the first solvation sphere only (five or six molecules of water), *dots* are related to the inclusion of COSMO model to the first solvation sphere and the *dashed line* is representing the full cluster containing 30 water molecules

between the average A_{FC} values are about 4.5 Gauss, which makes *ca* 5 % of average NR A_{FC} values. Nevertheless, the oscillations of A_{FC} values during the MDS are in the range of -15 to -110 Gauss, see Fig. 6. This shows, that the instant A_{FC} values are strongly correlating with the motion of the first solvation sphere molecules. As mentioned above, average A_{FC} values of the five coordinated Cu^{2+} correlate better with the A_{FC} values of the optimized $[Cu(H_2O)_6]^{2+}$ complex rather with A_{FC} values of $[Cu(H_2O)_5]^{2+}$ complex. This disagreement can be caused by changing of the shape of the Cu^{2+} coordination polyhedron related to the motion of the system during the MDS [13], which cannot be considered strictly a square pyramid (Berry pseudo-rotation).

The average REL HFCC values of five and six coordinated Cu^{2+} for B3LYP and M06 MDS geometries, respectively, are presented in Table 2. While HFCC values of the five coordinated Cu^{2+} (-15.6 and -15.3 Gauss for I5 and I6 system, respectively) correspond to each other well, in the case of the six coordinated Cu^{2+} (-12.7 and -21.5 Gauss for I5 and I6 system, respectively) the agreement is less convincing. Nevertheless, the difference between the particular values of six coordinated Cu^{2+} (8.8 Gauss) is smaller than their standard deviations (11.8 and 13.0 Gauss in the case

of I5 and I6 system, respectively, see also Table 2). Furthermore, one can see a considerable shift between the NR A_{FC} and the REL A_{iso} values, for both the time dependence as well as their averages, see Fig. 7 and Table 2. The calculated isotropic HFCC reported by Almeida et al. [26] is -15.5 Gauss in the case of the optimized geometry of the $[Cu(H_2O)_6]^{2+}$ complex (Ci symmetry) and -21.8 Gauss in the case of the $[Cu(H_2O)_5]^{2+}$ complex (denoted as "I"). The value of the experimental HFCC of copper(II) in water is -39.6 Gauss [27]. One can see that the calculated average HFCC of six coordinated I6 system (-21.5 Gauss) is the closest to the experimental value, although the best agreement with experiment in Almeida et al. [26] was obtained for $[Cu(H_2O)_5]^{2+}$ complex (-21.8 Gauss). On the other hand, the obtained average REL HFCCs of five coordinated I5 and I6 systems (-15.6 and -15.3 Gauss, respectively) are very close to the value of Almeida et al. [26] for $[Cu(H_2O)_6]^{2+}$ complex (-15.5 Gauss). Although this "agreement" is opposite to the expected one, it is also necessary to consider standard deviations of all calculated average REL HFCCs, see Table 2. These results point out again the large sensitivity of HFCC to the dynamics of the coordination polyhedron. Nonetheless, one can see that the importance of the proper evaluation of HFCC for solvated Cu^{2+} has to go beyond the Fermi contact interaction, and is actually untrusty without the spin-orbit effects [26, 29].

A detailed time evolution of the four-component HFCCs of six coordinated Cu^{2+} for a short time interval (*i.e.* 0.285 ps) is presented in Fig. 7, hand in hand with the NR HFCC values for comparison. Although the relativistic four-component values are changing rather quickly, they are corresponding well to the time evolution of the NR A_{FC}

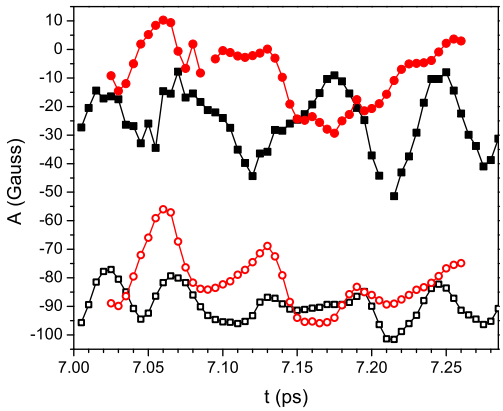

Fig. 7 Time evolution of relativistic (REL) B3LYP/UDZ hyperfine coupling constants (A_{iso}) and non-relativistic (NR) B3LYP/6-311g** Fermi contact terms (A_F) of six coordinated copper(II) of I5 and I6 systems from M06/6-31G MDS. The *black squares* are related to the I6 system (the full ones represent REL HFC constants and the empty one represent the NR HFC values) and the *red circles* are related to the I5 system (the full ones for REL HFC and the empty ones for the NR HFC values)

values. Only a few of the calculated A_{iso} values are not following the expected trends of the time dependence of NR A_{FC} values (check for instance the value at 7.08 ps in the case of system I5 in Fig. 7). These oscillations have to be assigned to some numeric and/or convergence issues at the four-component level of theory. Note that, the average A_{iso} values of six coordinated Cu atom for this short time interval are -7.0 and -24.6 Gauss for the I5 and I6 systems, respectively.

As was already mentioned in the Introduction section, the actual EPR measurement was performed at -10 $°C$ to obtain the hyperfine splitting in the EPR spectrum, and still the data is not well resolved [27]. Actually, hyperfine structure of the EPR spectra of Cu^{2+} in water is not resolved at room temperature at all. From this prospect, the average A_{iso} values based on the MDS trajectories are indeed close to zero, i.e. for the six coordinated I5 and for both five coordinated systems a zero A_{iso} value is within the standard deviation interval (σ). In the case of six coordinated I6 system two times σ has to be taken. Despite that, only one trajectory for each system (five and six coordinated I5 as well as I6) has been considered (accounting for a quite short time interval), the average A_{iso} values indeed indicate that the hyperfine interaction of Cu^{2+} in water at room temperature is not resolved.

Conclusions

Although, the systems of our interest (I5 and I6) had a different coordination number (5 and 6, respectively) of water molecules around copper(II) (Cu^{2+}) at the beginning of molecular dynamics simulations at 300 K, at the end of the MDS both independent trajectories prefer the same coordination which is closely related to the DFT functional used. The M06 MDS prefer rather the six coordinated Cu^{2+}. The transition from fivefold to sixfold coordination was observed after *ca* 3.5 ps of the M06/6-31G MDS at the temperature of 300 K, see Fig. 2a. On the other hand, B3LYP MDS prefer almost exclusively the fivefold coordination of Cu^{2+}. In the case of the BLYP 300 K MDS, the fivefold coordination is also preferred, although one of BLYP MD trajectories contained a four coordinated Cu^{2+} for about 3 ps. Nevertheless, the usage of a rather small double-zeta quality basis set in the MDS is an important factor which might have affected the resulting coordination number, hand in hand with the fact that the simulations were performed in a bulk accounting roughly for the second solvation sphere. We have to stress that the relatively short MDSs of the bulk systems (presented herein) have also their limits. Additional MDSs of a larger bulk, which accounted for polarization functions in the basis set, have led to the same conclusions about the sixfold and fivefold

coordination of Cu^{2+} in the M06/6-31g* and B3LYP/6-31g* trajectories, respectively. The obtained results lead to a different conclusion about the coordination number of Cu^{2+} at the B3LYP level of theory with respect to the work of Rode and coworkers [21–23] which seems to be stimulating for further activity in this regards on the theoretical battle field. In the case of the M06/6-31G MDSs at 350 K, a dynamic change of the number of the solvent molecules in the first solvation sphere is found and the coordination number is reversibly changing from five to six.

The average non-relativistic (NR) Fermi contact terms of five and six coordinated Cu^{2+} for the obtained MD trajectories (including first, second solvation sphere or COSMO) were found similar to each other, all values are from the interval of -89 to -83 Gauss (see Table 2). Although the individual A_{FC} values of particular MD geometries are in the range -110 to -15 Gauss. The situation is different in the case of the relativistic (REL) hyperfine coupling values. The time average REL HFCC values are from the interval -12 to -22 Gauss for all studied systems and their time dependence as well as average values (see Fig. 7 and Table 2) are considerably shifted from the NR Fermi contact values (see Fig. 6). Thus, the proper evaluation of the HFCC (including not only the FC term, but also SO effects - at least perturbatively) is superior already in the case of Cu^{2+} containing systems as has been already reported by Neese [29] or Almeida et al. [26]. The average relativistic HFCC values obtained for the two sets of geometries from the 300 K MDS are in line with the fact that at room temperature becomes the hyperfine structure of Cu^{2+} in water smeared out.

Supplementary material Supplementary material contains complete set of geometries from all the 300 K MDSs in the form of xyz files.

Acknowledgments First of all, we are very grateful for help, valuable discussions and know-how (via providing the ReSpect code) to Vladimír G. Malkin, Oľga L. Malkina (Slovak Academy of Science) and Michal Repiský (University of Tromsø). The financial support was obtained from APVV (contract No. APVV-0202-10) and VEGA (contracts No. 1/0327/12 and 1/0765/14). We are grateful to the HPC center at the Slovak University of Technology in Bratislava, which is a part of the Slovak Infrastructure of High Performance Computing (SIVVP project, ITMS code 26230120002, funded by the European region development funds) for the computational time and resources made available.

Conflict of interests The authors declare that they have no conflict of interest.

References

1. Lippard SJ, Berg JM (1994) Principles of Bioinorganic Chemistry. University Science Books, Mill Valley
2. Bertini I, Gray HB, Stiefel EI, Valentine JS (2007) Biological Inorganic Chemistry. University Science Books, Mill Valley
3. Falconi M, Iacovelli F, Desideri A (2013) J Mol Model 19:3695
4. Boča R, Hvastijová M, Kožíšek J, Valko M (1996) Inorg Chem 35:4794
5. Jia LF, Fu WF, Yu MM, Cao QY, Zhang JF, Yin Q (2005) Inorg Chem Commun 8:647
6. Bérces A, Nukada T, Margl P, Ziegler T (1997) J Mol Struct 397:121
7. Stace AJ, Walker NR, Firth S (1997) J Am Chem Soc 119:10239
8. Allen FH (2002) Acta Cryst B 58:380
9. Conquest v1.17, csd v5.36 (nov 2014). Copyright CCDC 2014
10. Frank P, Benfatto M, Szilagyi RK, D'Angelo P, Longa SD, Hodgson KO (2005) Inorg Chem 44:1922
11. Benfatto M, D'Angelo P, Della Longa S, Pavel NV (2002) Phys Rev B 65:174205
12. Persson I, Persson P, Sandström M, Ullström AS (2002) J Chem Soc Dalton Trans 7:1256
13. Pasquarello A, Petri I, Salmon PS, Parisel O, Car R, Tóth E, Powell DH, Fischer HE, Helm L, Merbach AE (2001) Science 291:856
14. Chaboy J, Muñoz-Páez A, Merkling PJ, Marcos ES (2006) J Chem Phys 124:064509
15. Breza M, Biskupič S, Kožíšek J (1997) J Mol Struct 397:121
16. Car R, Parrinello M (1985) Phys Rev Lett 55:2471
17. Laasonen K, Pasquarello A, Car R, Lee C, Vanderbilt D (1993) Phys Rev B 47:10142
18. Amira S, Spångberg D, Hermansson K (2005) Phys Chem Chem Phys 7:2874
19. Texler NR, Rode BM (1995) J Phys Chem 99:15714
20. Marini GW, Liedl KR, Rode BM (1999) J Phys Chem A 103:11387
21. Schwenk CF, Rode BM (2003) J Chem Phys 119:9523
22. Schwenk CF, Rode BM (2003) Comp Phys Commun 4:931
23. Moin ST, Hofer TS, Weiss AKH, Rode BM (2013) J Chem Phys 139:014503
24. Blumberger J, Bernasconi L, Tavernelli I, Vuilleumier R, Sprik M (2004) J Am Chem Soc 126:3928
25. de Almeida KJ, Murugan NA, Rinkevicius Z, Hugosson HW, Vahtras O, Ågren H, Cesar A (2009) Phys Chem Chem Phys 11:508
26. de Almeida KJ, Rinkevicius Z, Hugosson HW, Ferreira AC, Ågren H (2007) Chem Phys 332:176
27. Lewis WB, Alei JM, Morgan LO (1966) J Chem Phys 44:2409
28. Rinkevicius Z, Telyatnyk L, Sałek P, Vahtras O, Ågren H (2004) J Chem Phys 121:7614
29. Neese F (2003) J Chem Phys 118:3939
30. Alder BJ, Wainwright TE (1957) J Chem Phys 27:1208
31. Kutzelnigg W (2002) Chapter 12. Perturbation theory of relativistic effects in Relativistic Electronic Structure Theory. Part I. Fundamentals. Elsevier, Amsterdam, p 664
32. Pyykkö P (1971) Phys Lett A 35:53
33. Komorovský S, Repiský M, Malkina OL, Malkin VG, Ondík IM, Kaupp M (2008) J Chem Phys 128:104101
34. Repiský M, Komorovský S, Malkin E, Malkina OL, Malkin VG (2010) Chem Phys Lett 488:94
35. Malkin E, Repiský M, Komorovský S, Mach P, Malkina OL, Malkin VG (2011) J Chem Phys 134:044111

36. Malkin V, Malkina O, Reviakine R, Arbuznikov A, Kaupp M, Schimmelpfennig B, Malkin I, Repiský M, Komorovský S, Hrobarik P, Malkin E, Helgaker T, Ruud K (2012) ReSpect Program. Version 3.2.0, 2012
37. Lee C, Yang W, Parr RG (1988) Phys Rev B 37:785
38. Becke AD (1988) Phys Rev A 38:3098
39. Becke AD (1993) J Chem Phys 98:5648
40. Vosko SH, Wilk L, Nusair M (1980) Can J Phys 58:1200
41. Stephens PJ, Devlin FJ, Chabalowski CF, Frisch MJ (1994) J Phys Chem 98:11623
42. Zhao Y, Truhlar DG (2006) J Chem Phys 125:194101
43. Hehre WJ, Ditchfield R, Pople JA (1972) J Chem Phys 56:2257
44. Rassolov VA, Pople JA, Ratner MA, Windus TL (1998) J Chem Phys 109:1223
45. Krishnan R, Binkley JS, Seeger R, Pople JA (1980) J Chem Phys 72:650
46. Wachters AJH (1970) J Chem Phys 52:1033
47. Dunning JTH (1989) J Chem Phys 90:1007
48. Balabanov NB, Peterson KA (2006) J Chem Phys 125:074110
49. Miertus S, Scrocco E, Tomasi J (1981) Chem Phys 55:117
50. Barone V, Cossi M, Tomassi J (1997) J Chem Phys 107:3210
51. Frisch MJ, Trucks GW, Schlegel HB, Scuseria GE, Robb MA, Cheeseman JR, Scalmani G, Barone V, Mennucci B, Petersson GA, Nakatsuji H, Caricato M, Li X, Hratchian HP, Izmaylov AF, Bloino J, Zheng G, Sonnenberg JL, Hada M, Ehara M, Toyota K, Fukuda R, Hasegawa J, Ishida M, Nakajima T, Honda Y, Kitao O, Nakai H, Vreven T, Montgomery Jr JA, Peralta JE, Ogliaro F, Bearpark M, Heyd JJ, Brothers E, Kudin KN, Staroverov VN, Kobayashi R, Normand J, Raghavachari K, Rendell A, Burant JC, Iyengar SS, Tomasi J, Cossi M, Rega N, Millam JM, Klene M, Knox JE, Cross JB, Bakken V, Adamo C, Jaramillo J, Gomperts R, Stratmann RE, Yazyev O, Austin AJ, Cammi R, Pomelli C, Ochterski JW, Martin RL, Morokuma K, Zakrzewski VG, Voth GA, Salvador P, Dannenberg JJ, Dapprich S, Daniels AD, Farkas, Foresman JB, Ortiz JV, Cioslowski J, Fox DJ (2009) Gaussian.09 Revision D.01. Gaussian Inc., Wallingford CT
52. Berendsen HJC, van der Spoel D, van Drunen R (1995) Comp Phys Commun 91:43
53. Valiev M, Bylaska EJ, Govind N, Kowalski K, Straatsma TP, van Dam HJJ, Wang D, Nieplocha J, Apra E, Windus TL, de Jong WA (2010) Comp Phys Commun 181:1477
54. Berendsen HJC, Postma JPM, van Gunsteren WF, Nola AD, Haak JR (1984) J Chem Phys 81:3684
55. Klamt A, Schüürmann G (1993) J Chem Soc Perkin Trans 2:799
56. Visscher L, Dyall KG (1997) Atom Data Nucl Data Tabl 67:207
57. Allen MP, Tildeslay DJ (1987) Computer Simulation of Liquids. Clarendon Press, Oxford